Progress In Electromagnetics Research B, Vol. 59, 31–44, 2014

Feasibility Investigation of Low Cost Substrate Integrated Waveguide (SIW) Directional Couplers

Tiziana Castellano[1], Onofrio Losito[1], Luciano Mescia[1], Michele A. Chiapperino[1], Giuseppe Venanzoni[1], Davide Mencarelli[1], Giacomo Angeloni[2], Chiara Renghini[2], Pasquale Carta[2], and Francesco Prudenzano[1, *]

Abstract—In this paper, the feasibility of Substrate Integrated Waveguide (SIW) couplers, fabricated using single-layer TACONIC RF-35 dielectric substrate is investigated. The couplers have been produced employing a standard PCB process. The choice of the TACONIC RF-35 substrate as alternative to other conventional materials is motivated by its lower cost and high dielectric constant, allowing the reduction of the device size. The coupler requirements are 90-degree phase shift between the output and the coupled ports and frequency bandwidth from about 10.5 GHz to 12.5 GHz. The design and optimization of the couplers have been performed by using the software CST Microwave Studio©. Eight different coupler configurations have been designed and compared. The better three couplers have been fabricated and characterized. The proposed SIW directional couplers could be integrated within more complex planar circuits or utilized as stand-alone devices, because of their compact size. They exhibit good performance and could be employed in communication applications as broadcast signal distribution and as key elements for the construction of other microwave devices and systems.

1. INTRODUCTION

In recent years several Substrate Integrated Waveguide (SIW) devices such as antennas [1–3], filters, SIW-microstrip transitions [1, 4–6] and couplers [3, 4, 7, 8] have been reported in literature. SIW technology is a good technique for designing and fabricating microwave and millimeter-wave devices and circuits [9–24].

There is an evident similarity between the electromagnetic field distribution in a SIW and that occurring in conventional rectangular waveguides [10]. Therefore, microwave components designed in SIW technology offer very interesting performance. Fast prototyping and precise manufacturing, typical of standard printed circuit board (PCB) process, such as the use of single-layer dielectric substrate with metallic vias allow well known advantages, as rectangular-like wave guiding properties, compact size and high integration in complex planar circuits [11].

Many papers [8, 12, 13, 19–24] report couplers made using substrates with dielectric constants from $\varepsilon_r = 2.08$ to $\varepsilon_r = 2.94$ (e.g., Duroid) and exhibiting excellent characteristics. For example, in [8] Duroid single-layer planar directional couplers based on substrate integrated waveguide (SIW) technology have been presented. Prototypes of 3 dB, 6 dB and 10 dB SIW directional couplers have been totally realized in single-layer dielectric substrate with metallic vias, and fabricated using a standard PCB process. The SIW couplers have shown good performances with broad operation bandwidth, low insertion loss, low return loss and high isolation. In [19] a half mode substrate integrated waveguide (HMSIW) 3 dB coupler has been proposed. The HMSIW Duroid coupler has exhibited better characteristics than those obtained by using conventional SIW technique, i.e., lower insertion loss, larger bandwidth, higher

Received 8 January 2014, Accepted 10 March 2014, Scheduled 13 March 2014

* Corresponding author: Francesco Prudenzano (prudenzano@poliba.it).

[1] DEI — Dipartimento di Ingegneria Elettrica e dell'Informazione, Politecnico di Bari, Via E. Orabona 4 Bari, 70125, Italy. [2] R&D Department, Somacis Spa, Via Jesina 17, Castelfidardo 60022, Italy.

compactness (nearly half of size). Moreover, it has exhibited S_{11} parameter below $-15\,\mathrm{dB}$ in the frequency range from 9 GHz to 11 GHz and a phase difference between the coupled and the output ports of $92.5^\circ \pm 2.5^\circ$. In [24] two double layer SIW-based couplers have been proposed: a longitudinal-slots-based broad wall SIW coupler and its corresponding half mode SIW coupler. Coupling has been obtained through a set of narrow and offset slots, providing a wide coupling dynamic range. Isolation and input reflection characteristics better than 15 dB and 13 dB, respectively, were demonstrated over 24% fractional bandwidth at 12.5 GHz.

This paper reports the design and characterization of couplers using a low cost substrate material having dielectric constant ($\varepsilon_r = 3.5$). Moreover, a bandwidth of about 2 GHz, from about 10.5 GHz to 12.5 GHz (satellite and communication applications), and 90-degree phase shift between the output and coupled ports are required. Eight different directional couplers are designed by coupling two SIWs through an aperture in the common wall. The selection of TACONIC RF-35 as substrate material, allows a good trade-off between low cost and good performance. The coupler geometries (shapes), the size and the spacing of the vias have been varied and after an high number of simulations the optimized parameters have been identified. The better three optimized couplers have been fabricated and characterized. The design has been performed by employing the CST Microwave Studio© software, and the SIW couplers have been fabricated with a single-layer PCB process in SOMACIS plant.

The work is an extensive investigation on the feasibility of low cost TACONIC RF-35 couplers, in the X-band.

The paper is organized as follows in Section 2 a recall of the basic theory, in Section 3 the design of eight different couplers, in Section 4 fabrication an characterization of three promising devices.

2. FUNDAMENTALS OF THEORY

A well-known implementation of four ports directional couplers is obtained by electromagnetic coupling of two waveguides having a common wall, via a suitable aperture [15]. The coupling coefficient C is given by:

$$C = 10\log\left(\frac{1}{|S_{13}|^2}\right) = -20\log|S_{13}| \tag{1}$$

The propagation modes of a SIW strongly resemble to TE_{n0} modes of the rectangular waveguide. In particular, the fundamental mode is similar to the TE_{10}. TM modes cannot exist in the SIW because the gaps between metal vias do not allow longitudinal surface current. Moreover, the gaps cause a strong radiation, preventing the propagation of TM modes [14, 15]. Other important factors to be taken into account in the design of SIW structures are the size and the bandwidth.

The cutoff frequency f_c of a SIW can be determined via an empirical formulas [8, 14]:

$$f_c = \frac{c}{2\sqrt{\varepsilon_r}}\left(W_{SIW} - \frac{d_{via}^2}{0.95 \times s_{via}}\right)^{-1} \tag{2}$$

where c is the light speed in vacuum, ε_r the dielectric permittivity of substrate, d_{via} the diameter of metal vias, W_{SIW} the transverse via-to-via spacing, and s_{vias} the longitudinal via-to via spacing. The expression in parenthesis is the width of an equivalent rectangular waveguide [9]. This empirical formula is very accurate when:

$$\frac{d_{via}}{W_{SIW}} < 0.2 \tag{3}$$

There are three loss mechanisms in SIW structures [17]: conductor losses, due to the finite conductivity of the metal walls, dielectric material losses radiation and scattering losses due to the metal vias.

Negligible radiation losses occur when metal vias are large enough and closely spaced. In this case, the SIW electromagnetic modes tend to be almost completely bounded, as in a classical rectangular waveguide. In particular, in the design the following condition has been considered:

$$\frac{s_{via}}{d_{via}} < 2.5 \tag{4}$$

In this way, the attenuation constant due to radiation loss is smaller than 1 dB/m [15].

A transition from microstrip waveguide to SIW is designed by matching the input impedance between SIW and the 50 Ω input microstrip impedance.

According to the design process mentioned in [14], H-plane geometric variation of side wall are employed to achieve impedance matching. The aperture in the common wall determines the bandwidth performance of the coupler. However, it is possible to improve the bandwidth by increasing the aperture size. This approach is qualitative and it is simply derived as an approximated extension of the theory applied to the conventional (not SIW) channel waveguides coupled by apertures. It is introduced to justify the design strategy followed in the numerical simulations illustrated in Section 3. A tradeoff between good bandwidth (about 2 GHz) a small size (a few centimeters) is a design goal. Moreover, a further SIW coupler requirement is a phase difference of 90-degree between the S_{12} and S_{13} scattering parameters over the whole bandwidth.

3. DESIGN

For all the eight designed SIW couplers the substrate material is TACONIC RF-35, with relative dielectric permittivity $\varepsilon_r = 3.5$. Two different thicknesses $h_1 = 1.52$ mm and $h_2 = 0.5$ mm have been considered. Layers having these thicknesses are available on market.

The metallic vias of the side wall have diameter d_{via}, offset via distance from the the side wall is d_{lvia}, and center to center space S_{via}. The metallic vias of SIW coupler common central wall have diameter c_{via} and center to center distance S_{cvia}. The aperture in the common SIW walls has width W_a. This aperture width as well as the central metallic vias are used to control the coupling between input and coupled ports (Figure 1).

The SIW couplers are designed by employing an high number metallic vias (in the range from $N = 74$ to $N = 152$) in the dielectric substrate. More precisely, by fixing for each coupler the same

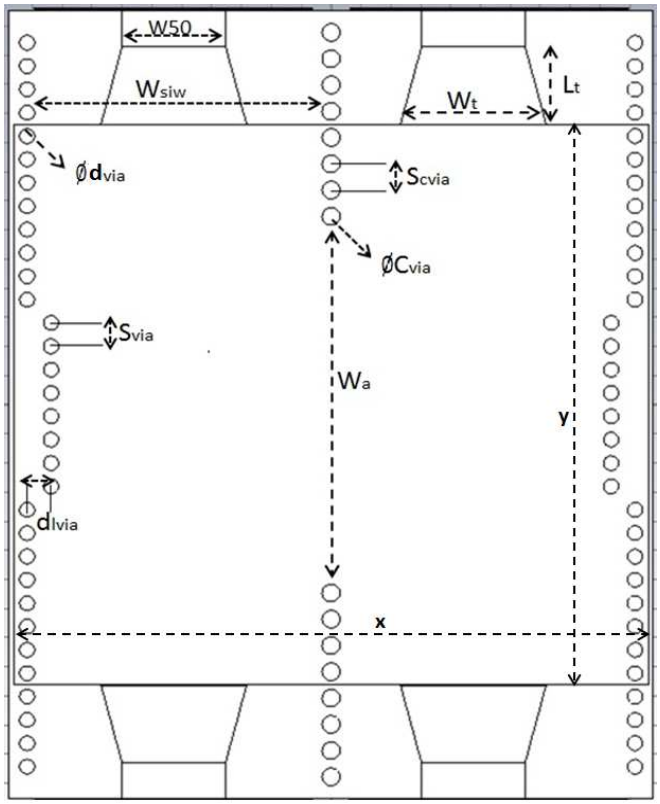

Figure 1. Front section of SIW coupler.

substrate size, including the feeding microstrips, and by imposing the conditions of Eq. (3) and Eq. (4), the different geometries #1–#8, having walls with various shapes and lengths, have required a suitable number of vias, depending on the particular layout, e.g., $N = 74$ for #5 coupler, $N = 90$ for #8 coupler and 152 for #3 coupler. The couplers #1–#4 have been designed considering a TACONIC RF-35 substrate thickness of $h = 0.50\,\text{mm}$ while for the couplers #5–#8 TACONIC RF-35 substrate thickness is $h = 1.52\,\text{mm}$.

More precisely, in the design the starting geometry of coupler, i.e., the shape but not the sizes, was inspired by literature with reference to couplers optimized for other materials [8, 12, 18] since TACONIC RF-35 is less used for this kind of devices. After a rough choice of the SIW geometrical parameters, made by employing the equivalent rectangular waveguide model reported in the theory, the geometric parameters of each SIW directional coupler has been optimized via the full-wave electromagnetic solver CST Microwave Studio©. In particular, by exploiting Eq. (2), the SIW width of about $W_{siw} = 10\,\text{mm}$ for the chosen cutoff frequency $f_c = 9\,\text{GHz}$ has been calculated; f_c has been identified below the operation bandwidth, i.e., 10.5 GHz–12.5 GHz. The choice of d_{via} and s_{via} has been performed according to Eq. (3) and Eq. (4). Therefore, the sizes of the coupled TACONIC RF-35 waveguides have been approximately identified. By considering a qualitative aspect ratio x/y by literature [8] the coupler length of about $y = 19\,\text{mm}$ has been considered; then the CST numerical optimization has been necessary because of the coupler complex geometries and since the coupled waveguides are not exactly rectangular ones, but differently shaped (Eq. (2) cannot be rigorously applied). The approach in the design has been the following one: i) to consider the state of the art of the geometries optimized for other materials, reported in literature; ii) adapt the geometries inspired by literature to the low cost TACONIC RF-35 layers, having available on market thicknesses $h_1 = 0.5\,\text{mm}$ and $h_2 = 1.52\,\text{mm}$; iii) modify the wall shapes in order to enhance the coupling coefficient C, by guiding the electromagnetic field in the coupled waveguides; iv) provide a good isolation between port 1 and 4, less than about $-15\,\text{dB}$; v) maintain the geometrical symmetry of the couplers; vi) provide the coupler operation in the desired bandwidth. The metalized via holes outside the SIW, close to the feeding microstrips, constitute a further optimization of the coupler design. They have been designed in order to reduce the leak of electromagnetic field due to the SIW to microstrip transition, by enhancing the electromagnetic bounding. Their effect on the electromagnetic field bounding is quite similar for all the eight investigated couplers 1#–8#. For shortness it will be shown in detail only for the coupler 8#. The coupler geometric variations, investigated or employed in the design, are briefly summarized before their extensive description. Starting from the simplest geometry of coupler #1, Figure 2(a), and coupler #5, Figure 6(a), the coupler shapes have been changed by following two different ideas: i) to employ suitable rows of metalized holes in offset position with respect to the side walls, as for couplers #2, #3, #4, #6, see Figures 3(a), 4(a), 5(a), 7(a), respectively; ii) to design smooth variations of the side walls, minimizing the losses, as for couplers #7, #8, see Figures 8(a) and 9(a), respectively. Both these strategies i) and ii) allow

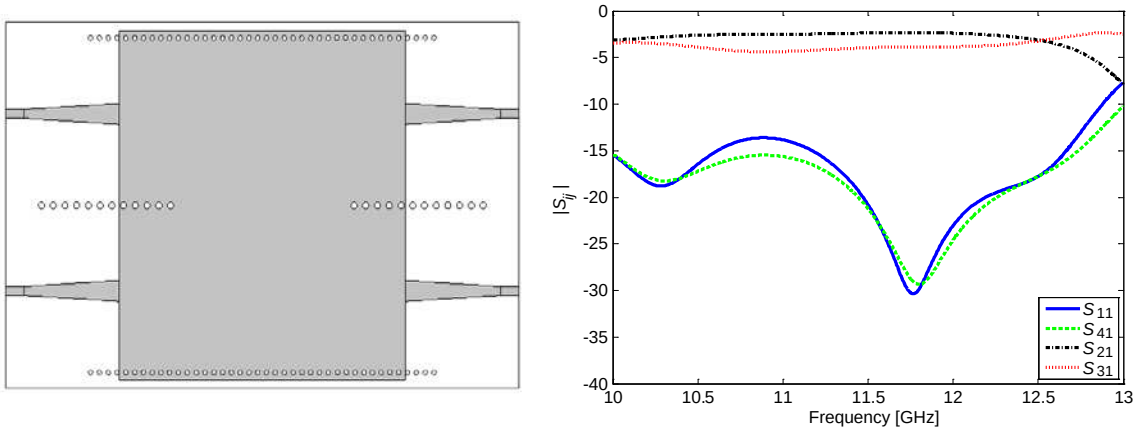

Figure 2. (a) Front section view of coupler #1. (b) Coupler #1 S-parameters versus frequency.

Table 1. Optimal coupler parameters.

	#1	#2	#3	#4	#5	#6	#7	#8
c_{via} (mm)	0.4	0.4	0.4	0.4	0.6	0.6	0.6	0.6
s_{cvia} (mm)	0.8	0.8	0.8	0.8	0.9	0.9	0.9	0.9
d_{via} (mm)	0.3	0.3	0.3	0.3	0.5	0.5	0.5	0.5
s_{via} (mm)	0.7	0.7	0.7	0.7	0.8	0.8	0.8	0.8
L_t (mm)	13	13	13	13	5.3	2.65	3.5	3.6
W_t (mm)	2.25	2.25	2.25	2.25	4.86	4.86	4.86	4.86
W_{50} (mm)	1.05	1.05	1.05	1.05	3.46	3.46	3.46	3.46
w_a (mm)	12.5	12.5	12.5	12.6	12.9	12.9	11.9	11.2
W_{SIW} (mm)	9.9	9.9	9.9	9.9	9.9	9.9	10.4	10.9
h (mm)	0.5	0.5	0.5	0.5	1.52	1.52	1.52	1.52
x (mm)	21	21	21	21.5	21.2	21.2	22.5	23
y (mm)	19.5	19.5	19.5	19.5	19.2	19.2	19	19.3
d_{lvia} (mm)	//	0.9	0.9	0.9	//	0.8	0.5	0.5

an electromagnetic field perturbation affecting the impedance matching, the coupling strength and the bandwidth operation.

Table 1 reports the optimal coupler parameters. The simulations highlight that when the coupling between the input port (1) and coupled port (3) becomes weak, both the moduli of S_{11} and S_{41} scattering parameters increase. To overcome this drawbacks, many guess solutions have been investigated, being inspired to the literature couplers made of other materials [8–12, 18]. Parametric variation of substrate (coupler) width x, substrate (coupler) length y, microstrip-to-SIW transition length L_t, microstrip-to-SIW transition width W_t, aperture width w_a, SIW width W_{SIW}, vias diameter c_{via} and d_{via}, via-to-via space s_{cvia}, s_{via}, and d_{lvia} (e.g., see Figure 1) have been performed via a number of simulations, with the aim of optimizing the coupler performance. Table 1 reports the optimized parameters in order to obtain couplers with a bandwidth of nearly 2 GHz, from about 10.5 GHz to 12.5 GHz, and 90-degree phase shift between the output and coupled ports are required. It is worthwhile to note that the simulated curves, reported in the following figures, refer to the optimized parameters of Table 1.

Figure 2(a) illustrates the front section view of the first designed coupler #1. It is geometrically similar to the SIW coupler reported in [8], fabricated on Duroid substrate. The optimized geometry parameters are reported in column #1 of Table 1. Figure 2(b) illustrates the simulated coupler scattering parameters S_{ij} for coupler #1. For the optimized coupler #1, S_{11} parameter is below -18 dB in the range from about 11.3 GHz to 12.6 GHz, S_{21} and S_{31} moduli are almost constant being close to -2.5 dB and -4 dB, from about 10.5 GHz to 12 GHz, respectively.

Reflections due to the common wall discontinuities at the ends of the coupling region, i.e., at the aperture ends, worsen the coupler characteristics. To overcome this drawback, couplers making use of continuous coupling between adjacent waveguides through a common full-height slot in the narrow wall have been proposed in [18, 23].

H-plane steps are employed to achieve impedance matching. The number of steps determines the bandwidth performance of the coupler [12, 18, 23]. In Figure 3(a), the coupler #2 is illustrated. It is obtained by adding rows of vias parallel to the coupler longitudinal axis close to the side walls.

The optimized geometry parameters are reported in column #2 of Table 1. The simulated scattering parameters for coupler #2 are illustrated in Figure 3(b). Differently from the results reported in literature for Duroid substrate (or other substrates having the same dielectric constant) [12, 23], the geometry of #2, when optimized for TACONIC RF-35, (or other substrates having the same dielectric constant) does not provide good performances. In fact, S_{11} modulus is higher than -10 dB for frequencies below 11 GHz and S_{31} modulus is lower than -5 dB from 10 GHz to 12.4 GHz.

Similar results (Figure 4(b)) are obtained by optimizing the geometry of coupler #3 (Figure 4(a)).

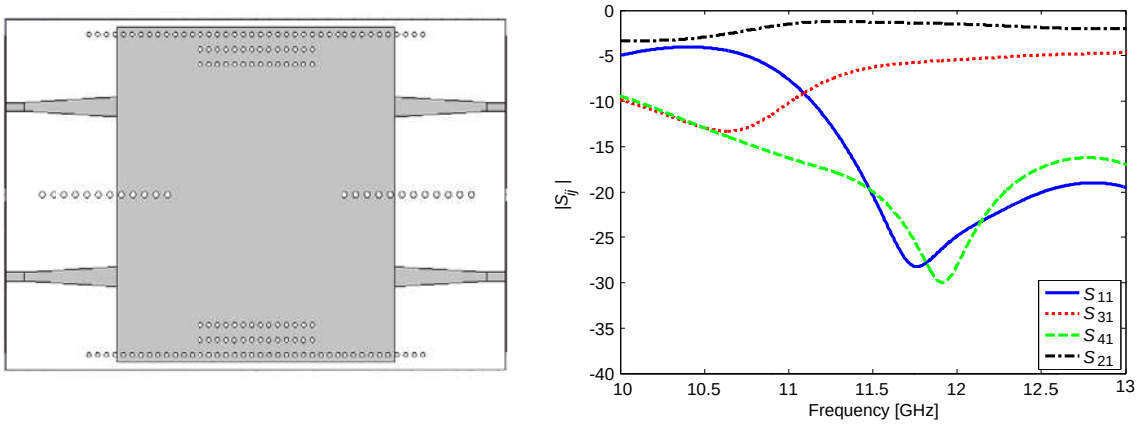

(a) (b)

Figure 3. (a) Front section view of coupler #2. (b) Coupler #2 *S*-parameters versus frequency.

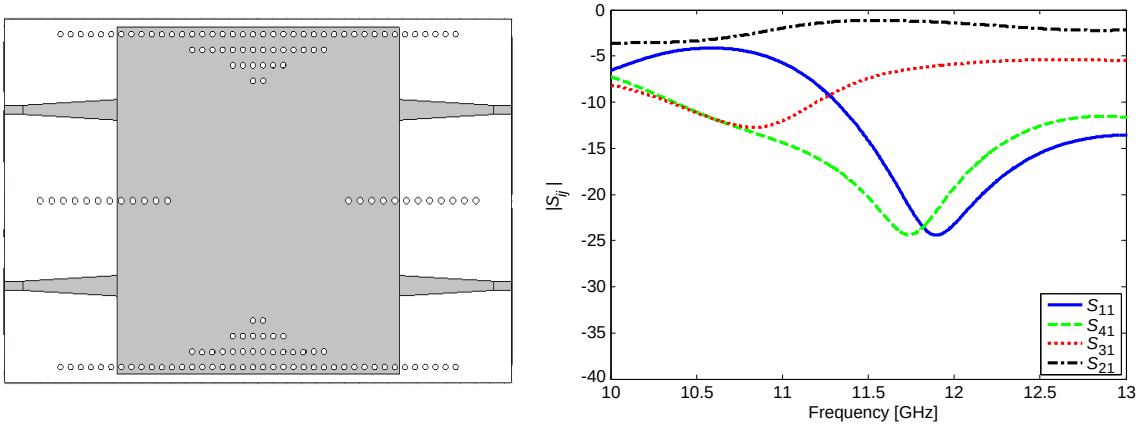

(a) (b)

Figure 4. (a) Front section view of coupler #3. (b) Coupler #3 *S*-parameters versus frequency.

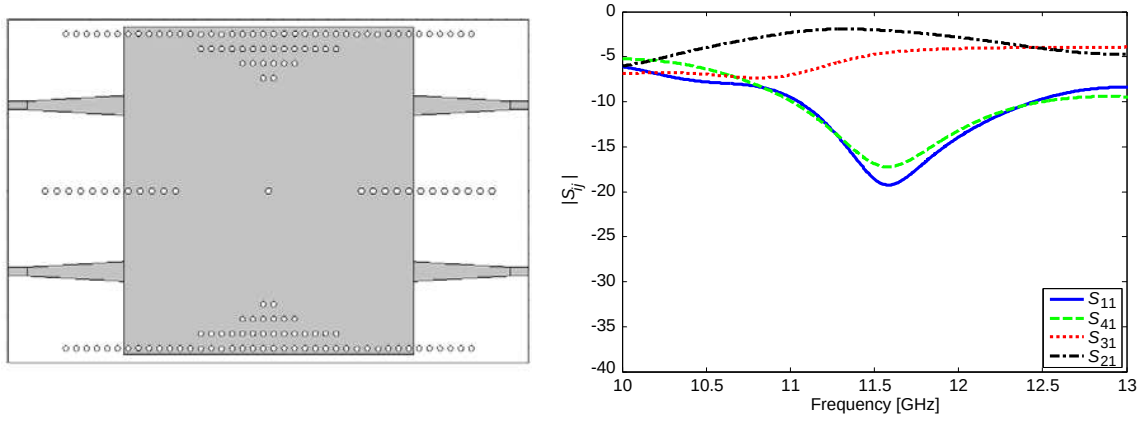

(a) (b)

Figure 5. (a) Front section view of coupler #4. (b) Coupler #4 *S*-parameters versus frequency.

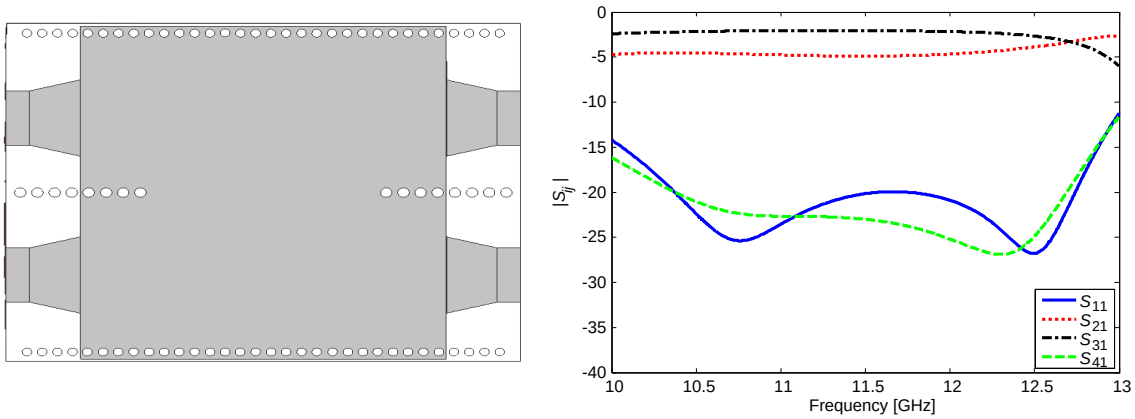

Figure 6. (a) Front section view of coupler #5. (b) Coupler #5 S-parameters versus frequency.

It is worthwhile to note that the geometries quite similar to the coupler #3 one, optimized for Duroid substrate, allow very good performance in both Ku and K bands [8, 12, 18, 23].

When the coupling between port 1 (input port) and port 3 (coupled port) becomes weak, the return loss and isolation response worsen. As a consequence, the design of a weak-coupling coupler using the configuration of couplers #1–#3 [8] is not trivial. To overcome this drawback, an extra central metallic via has been added, as for Duroid coupler in order to decrease the modulus of S_{11}, as proposed in [8]. Figure 5(a) illustrates the designed geometry for coupler #4. Also in this case, the coupler optimized with TACONIC RF-35 substrate material exhibits lower performances than those reported in literature for Duroid. In fact, in Figure 5(b), S_{11} modulus is higher than -10 dB below 11 GHz and it is lower than -14 dB for frequencies higher than 11.3 GHz, while the S_{11} parameters of the optimized Duroid coupler reported in [8] is lower than -20 dB.

The most promising coupler among those investigated is #1. The coupler #5, is obtained by refining of the same layout of #1 for a substrate thickness $h = 1.52$ mm. It is illustrated in Figure 6(a). The S_{11} parameter shows good performance, it is lower than -18 dB from about 10.4 GHz to 12.7 GHz, therefore over the whole frequency range of satellite communication. S_{31} and S_{21} moduli are close to -2 dB and to -4.5 dB, respectively (Figure 6(b)). The simulation indicates that coupler #5 has better performances than those of coupler #1.

Therefore, the optimization of other couplers #6–#8, by considering $h = 1.52$ mm has been performed. Coupler #6 is illustrated in Figure 7(a). It shows higher performance than coupler #5, the modulus of S_{21} and S_{31} scattering parameters are close to -2.5 dB and to -3.5 dB, respectively, over the whole frequency range (Figure 7(b)), S_{11} modulus is lower than -18 dB for frequencies higher than 10.2 GHz and, in particular, lower than -20 dB from 10.2 GHz to 11.6 GHz.

To mitigate the deleterious effect of sharp step change, a concave part of the side wall vias is designed with a smoother profile [14]. Better scattering parameters values have been obtained through a parametric analysis in which the parameter d_{via}, i.e., the distance of the inductive vias from the straight lateral wall of the coupler, has been varied leading to a suitably curved wall profile.

Coupler #7 is illustrated in Figure 8(a). The scattering parameters of coupler #7, after the parametric optimization, are shown in Figure 8(b). Good coupling performances are obtained. S_{11} and S_{31} moduli are slightly worse than those of coupler #6. In fact they are close to -2.5 dB and to -4.5 dB respectively. S_{11} modulus is lower than -15 dB for frequency higher than 10.6 GHz, in particular lower than -19 dB from about 10.6 GHz to 12 GHz.

Coupler #8 layout, shown in Figure 9(a), is not reported in literature. All the via walls are very smooth. In fact, both the via side walls and inductive posts (vias) of common central wall, have been obtained by optimizing the parameters d_{via} and W_{siw}. The scattering parameters are shown in Figure 9(b). S_{31} is slightly lower than that of coupler #6, being close to -4.5 dB, S_{21} is close to -2 dB. S_{11} modulus is lower than -18 dB, in the range frequency from 10.2 GHz to 11.7 GHz while it is lower than -15 dB until 12.5 GHz.

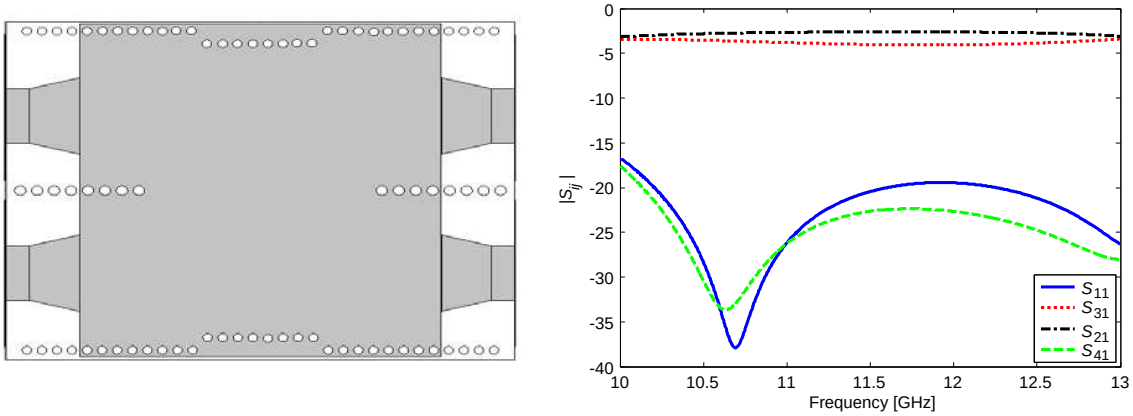

Figure 7. (a) Front section view of coupler #6. (b) Coupler #6 S-parameters versus frequency.

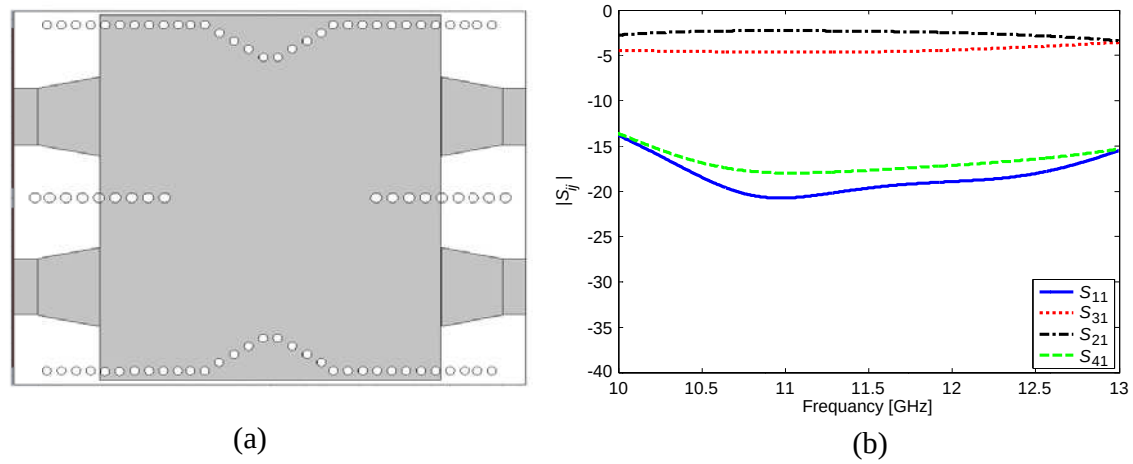

Figure 8. (a) Front section view of coupler #7. (b) Coupler #7 S-parameters versus frequency.

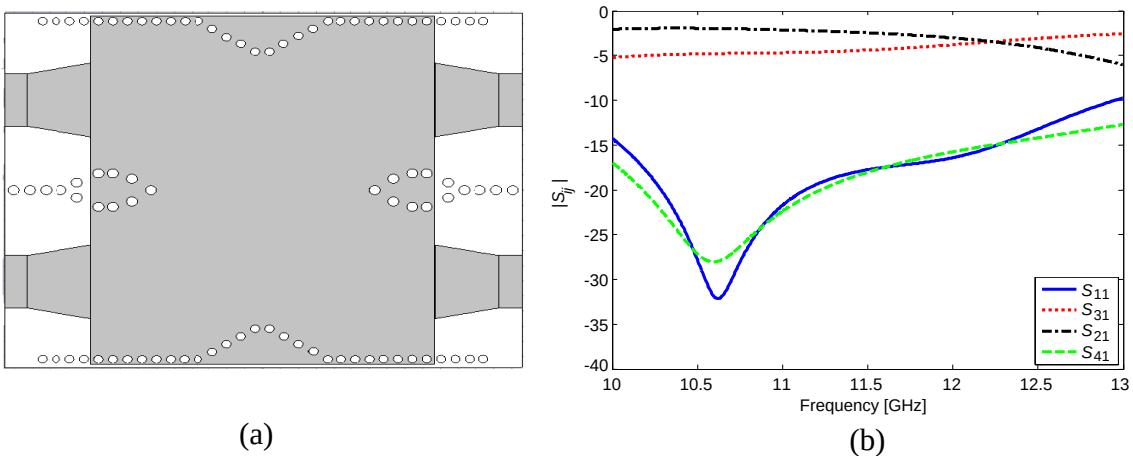

Figure 9. (a) Front section view of coupler #8. (b) Coupler #8 S-parameters versus frequency.

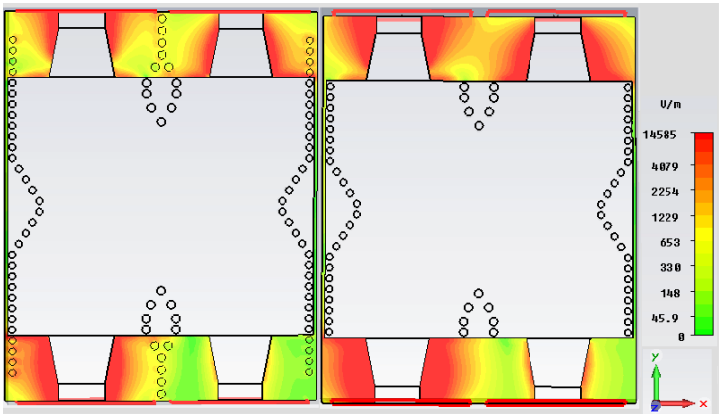

Figure 10. (a) Electric field amplitude in coupler #8, at $z = 0$ plane; (a) with and (b) without vias surrounding the microstrip transitions.

Suitable metalized holes surrounding the microstrip transitions have been reported in literature [8, 12, 14], they have been designed for the proposed couplers. As an example, their effect is well evidenced for coupler #8. More precisely, Figure 10 illustrates the distribution of the electric field amplitude, at the plane $z = 0$, for coupler #8 with (a) and (b) without metalized holes surrounding the microstrip transitions. In Figure 10(b) the electric field leakage near the microstrip transition is larger than in (a), where the via walls contribute to better bound the electric field distribution.

Table 2 reports the simulated couplers #1–#8 performances, where C is the coupling coefficient mean value, f_c is central frequency, S_{41} modulus is evaluated in the range from 10.5 GHz to 12.5 GHz. They have been obtained via the full-wave electromagnetic solver, CST Microwave Studio©.

Table 2. Simulated performance of couplers.

Coupler	C (dB)	h	$\lvert S_{41}\rvert$ (dB)	f_c (GHz)
#1	6.48	0.5	< -15	11.8
#2	16.83	0.5	< -15	11.8
#3	16.35	0.5	< -10	11.9
#4	10.52	0.5	< -10	11.6
#5	5.19	1.52	< -20	10.8
#6	5.35	1.52	< -20	10.7
#7	8.2	1.52	< -17	11
#8	7.41	1.52	< -16	10.7

4. COUPLER FABRICATION AND CHARACTERIZATION

Couplers 6#–8# have been fabricated by using a standard single-layer PCB process in SOMACIS. They are illustrated in Figure 11.

The corresponding measured scattering S_{11}, S_{12}, S_{13} parameters, utilizing a network analyzer Agilent N5224A, are illustrated in Figure 12. A good agreement with the simulations results was obtained. In fact, in all the three cases the couplers well operate in the desired frequency range.

Coupler #6 S measured parameters are illustrated in Figure 12(a). The modulus of S_{21} and S_{31} scattering parameters are close to -4 dB and to -5 dB, respectively, over the whole frequency range; S_{11} modulus is below -18 dB from 10.2 GHz to 11.6 GHz and it is lower than -17 dB for higher frequencies.

Coupler #7 S measured parameters are shown in Figure 12(b). The modulus of S_{21} and S_{31} scattering parameters are close to $-3.5\,\mathrm{dB}$ and to $-5\,\mathrm{dB}$, respectively, over the whole frequency range; S_{11} modulus is below $-17\,\mathrm{dB}$ from 10.7 GHz to 11.9 GHz and lower than $-16\,\mathrm{dB}$ for higher frequencies. Coupler #8 S measured parameters are depicted in Figure 12(c). The modulus of S_{21} and S_{31} scattering parameters are close to $-3.5\,\mathrm{dB}$ and to $-5.5\,\mathrm{dB}$, respectively, until 12.6 GHz, S_{11} modulus is below $-16\,\mathrm{dB}$ from 10.5 GHz to 12.3 GHz and it slightly increases for higher frequencies. Is worthwhile noting that, for

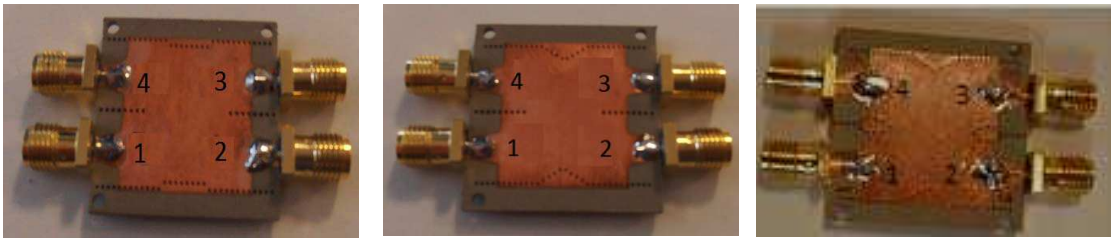

(a) (b) (c)

Figure 11. (a) Prototype coupler #6. (b) Prototype coupler #7. (c) Prototype coupler #8.

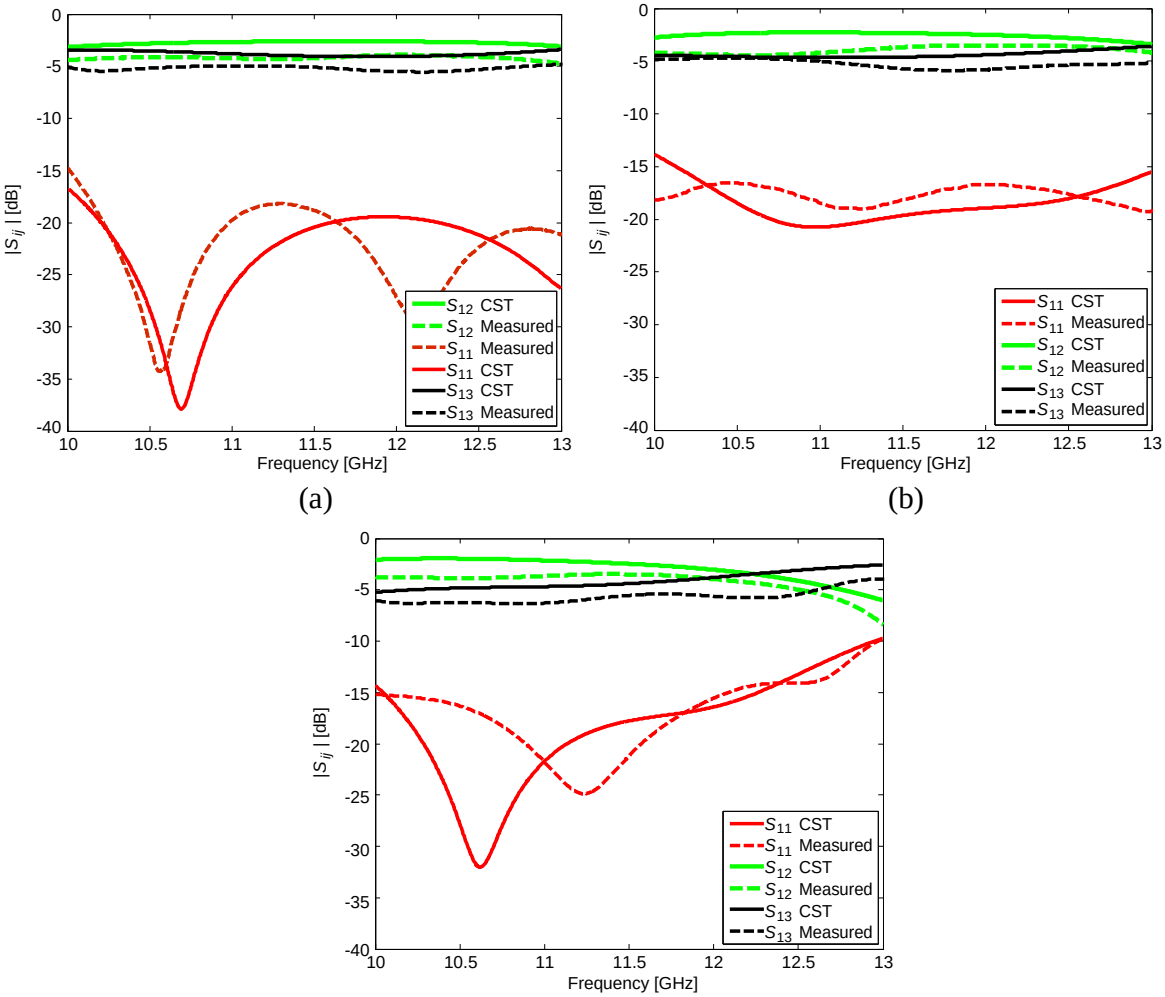

Figure 12. Comparison among simulated and measured S_{11}, S_{12}, S_{13} moduli of: (a) coupler #6; (b) coupler #7; (c) coupler #8.

Table 3. Measured performance of couplers.

Coupler Prototype	C (dB)	h	$\|S_{41}\|$ (dB)	f_c (GHz)
#6	9.8	1.52	< -18	10.6
#7	10.1	1.52	< -17	11.2
#8	10.2	1.52	< -16	11.2

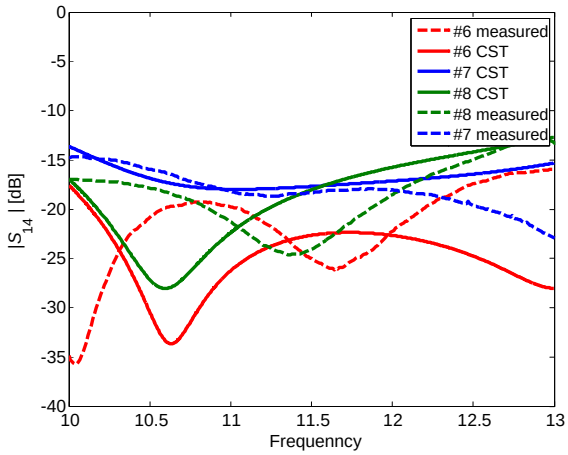

Figure 13. Comparison among simulated and measured S_{14} modulus of couplers #6, #7, #8.

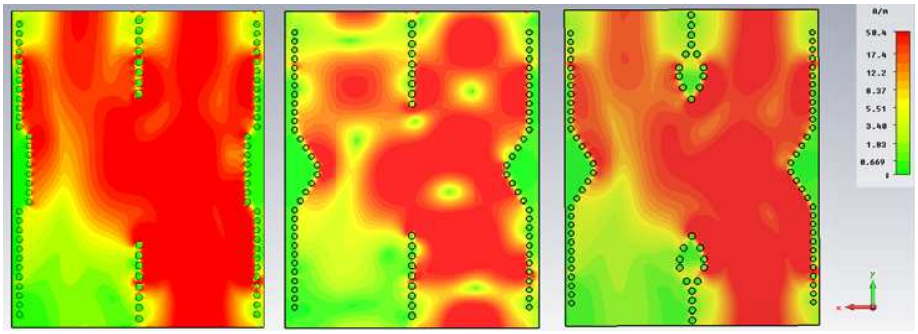

Figure 14. Surface current density at $z = 0$ metallic plane, frequency 11.5 GHz, for (a) coupler #6; (b) coupler #7; (c) coupler #8.

all the three fabricated couplers, in the bandwidth from 10.5 GHz to 12.5 GHz, the S_{11} modulus is lower than -15 dB. The differences between the magnitude of the S_{12} and S_{13} are not negligible ones. However, S_{12} and S_{13} moduli are typical values, reported in literature for SIW couplers designed as 3 dB power dividers [8, 13, 14, 19, 25].

Table 3 reports the measured performance of couplers #6–#8, where C is the coupling coefficient mean value, f_c is central frequency, S_{41} modulus is evaluated in the range from 10.5 GHz to 12.5 GHz.

Figure 13 illustrates the simulated and measured S_{14} parameters versus the frequency. The discrepancy among the simulated and the measured curves could be due to the employment of two small flexible 2.4 cables and two adapters (required in the measurement because of the reduced distance between the ports 1 and 4) which have been compensated in the measurement calibration via a software procedure. Anyway, it is worthwhile noting that in all the cases both measured and simulated curves

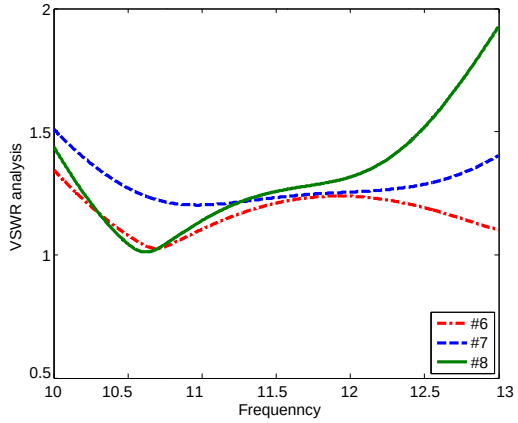

Figure 15. Voltage standing wave ratio (VSWR) versus the frequency for couplers #6; #7; #8.

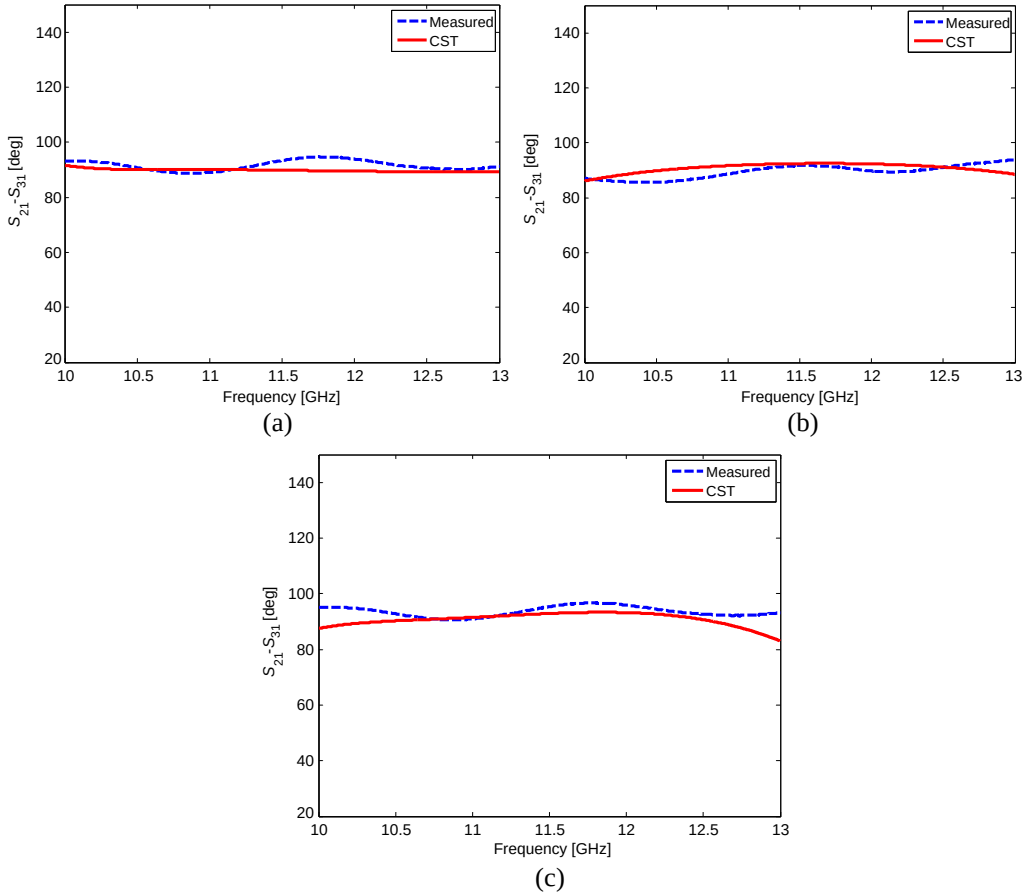

Figure 16. Comparison among simulated and measured phase difference of S_{21} and S_{31} of: (a) coupler #6; (b) coupler #7; (c) coupler #8.

are below about -15 dB in the range from 10.5 GHz to 12.5 GHz. Therefore, in all the three cases the measured S_{14} curves versus the frequency show a good coupler isolation between ports 1 and 4.

Figure 14 illustrates the distribution of the surface current density at $z = 0$ metallic plane, at the frequency 11.5 GHz, for (a) coupler #6; (b) coupler #7; (c) coupler #8. The operation of the couplers is apparent. The current distribution is more homogeneous for coupler #6 and coupler #8.

Figure 15 illustrates the voltage standing wave ratio (VSWR), calculated with respect to an impedance of 50 Ω, at the input port 1, versus the frequency. As expected, it is quite low, being below 1.5 and higher than the unit, in the range from 10.5 GHz to 12.5 GHz. This confirms the good impedance matching over the operation band. For symmetry, for each coupler #6; #7; #8, the other ports have the same behavior. The phase difference between S_{31} and S_{21} parameters, simulated and measured, are illustrated in Figure 16, for couplers #6-#7-#8. In all the three cases the abovementioned phase difference is close to 90°. Fabrication tolerances or simulation approximations, producing slight systematic phase errors on S_{12} and S_{13} separately (i.e., errors resulting from the measurement procedure or from the employed numerical methods), are compensated by the phase difference calculation (phase of S_{12}-S_{13}).

5. CONCLUSION

An extensive investigation on the feasibility of low cost TACONIC RF-35 couplers, in the X-band, has been performed. Three Substrate Integrated Waveguide (SIW) couplers, made of single-layer TACONIC RF-35 dielectric substrate have been fabricated by using a standard PCB process. The optimized couplers exhibit intriguing performances, comparable with those of SIW couplers made of higher cost substrates. As example, coupler #8 exhibits a phase difference of 90-degree, and coupling coefficient mean value $C = 10.2$ while the optimized coupler #7 exhibits a phase difference of 90-degree, and coupling coefficient mean value $C = 10.1$, both couplers exhibit a bandwidth of about 2 GHz in the wavelength range of satellite communication. The proposed couplers are promising candidates as low cost devices for microwave circuits. Potential market regards space, digital and broadcast satellite application.

ACKNOWLEDGMENT

This work has been partially supported within the MIUR plan: - PON01_01224 "Sviluppo di tecnologie in guida d'onda integrata (SIW) per applicazioni ICT a microonde"; - PONa3_00298 "Potenziamento delle strutture e delle dotazioni scientifiche e tecnologiche del polo scientifico e tecnologico Magna Grecia"; - PON02_00576 _3329762 DD MIUR n.818/Ric. Del 26/11/12 "Sistemi avanzati mini-invasivi di diagnosi e radioterapia" _AMIDERHA.

REFERENCES

1. Navarro, D. V., L. F. Carrera, and M. Baquero, "A SIW slot array antenna in Ku band," *IEEE Proceedings of the Fourth European Conference on Antennas and Propagation (EuCAP 2010)*, 1–4, 2010.
2. Losito, O., L. Mescia, D. Mencarelli, G. Venanzoni, and F. Prudenzano, "SIW cavity-backed patch antenna for Ku band applications," *7th European Conference on Antennas and Propagation (EUCAP 2013)*, 3095–3098, 2013.
3. Losito, O., L. Mescia, M. A. Chiapperino, T. Castellano, G. Venanzoni, D. Mencarelli, G. Angeloni, P. Carta, E. M. Starace, and F. Prudenzano, "X-band SIW cavity-backed patch antenna for radar applications," *European Microwave Conference 2013 (EuMW 2013)*, 199–202, 2013.
4. Cong, Z.-P., P. Wang, and P.-H. Li, "Analysis and experiment of transition between microstrip and a miniaturization substrate integrated waveguide (SIW)," *7th International Symposium on Antennas, Propagation & EM Theory, ISAPE' 06*, 1–4, Oct. 2006.
5. Deslandes, D. and K. Wu, "Integrated microstrip and rectangular waveguide in planar form," *IEEE Microwave Wirel. Compon. Lett.*, Vol. 11, No. 2, 68–70, 2001.
6. Hao, Z. C., W. Hong, J. X. Chen, X. P. Chen, and K. Wu, "Planar diplexer for microwave integrated circuits," *IEEE Proc. Microw. Antennas Propag.*, 455–459, 2005.
7. Castellano, T., O. Losito, L. Mescia, M. A. Chiapperino, G. Venanzoni, D. Mencarelli, G. Angeloni, C. Renghini, P. Carta, P. Potenza, and F. Prudenzano, "Substrate integrated waveguide fixed

phase shifter for 90°-degree directional coupler," *2013 IEEE Proceeding International Conference on Microwaves, Communications, Antennas and Electronic Systems (COMCAS 2013)*, 2013.

8. Hao, Z. C., W. Hong, J. X. Chen, H. X. Zhou, and K. Wu, "Single-layer substrate integrated waveguide directional couplers," *IEEE Proc. — Microwave Antennas Propagation*, Vol. 153, No. 5, 426–431, Oct. 2006.
9. Cassivi, Y., L. Perregrini, P. Arcioni, M. Bressan, K. Wu, and G. Conciauro, "Dispersion characteristics of substrate integrated rectangular waveguide," *IEEE Microw. Wireless Compon. Lett.*, Vol. 12, No. 2, 333–335, Feb. 2002.
10. Yan, L. and W. Hong, "Investigations on the propagation characteristics of the substrate integrated waveguide based on the method of lines," *IEEE Proc. — Microw. Antennas Propag.*, Vol. 152, No. 1, 35–42, 2005.
11. Zhang, Y. L., W. Hong, F. Xu, K. Wu, and T. J. Cui, "Analysis of guided wave problems in substrate integrated waveguides — Numerical simulations and experimental results," *IEEE MTT-S International Microwave Symposium Digest*, 2049–2052, Jun. 2003.
12. Bing, L., W. Hong, Z. C. Hao, and K. Wu, "Substrate integrated waveguide 180-degree narrow wall directional coupler," *IEEE APMC Proceedings*, Vol. 1, 2005.
13. Cheng, Y., W. Hong, and K. Wu, "Novel substrate integrated waveguide fixed phase shifter for 180-degree directional coupler," *IEEE/MTT-S International Microwave Symposium*, 189–192, Jun. 2007.
14. Han, L., K. Wu, X.-P. Chen, and F. He, "Accurate and efficient design technique for wideband substrate integrated waveguide directional couplers," *International Journal of RF and Microwave Computer-Aided Engineering*, Vol. 22, No. 2, 48–259, Wiley Periodicals, Inc., 2011.
15. Bozzi, M., F. Xu, D. Deslandes, and K. Wu, "Modeling and design considerations for substrate integrated waveguide circuits and components," *8th International Conference on Telecommunications in Modern Satellite, Cable and Broadcasting Services, TELSIKS 2007*, P-VII–P-XVI, Sep. 2007.
16. Xu, F. and K. Wu, "Guided-wave and leakage characteristics of substrate integrated waveguide," *IEEE Transactions on Microwave Theory and Techniques*, Vol. 53, No. 1, 66–73, Jan. 2005.
17. Xu, F., Y. Zhang, W. Hong, K. Wu, and T. J. Cui, "Finite difference frequency-domain algorithm for modeling guided wave properties of substrate integrated waveguide," *IEEE Transactions on Microwave Theory and Techniques*, Vol. 51, No. 11, 2221–2227, Nov. 2003.
18. Hildebrand, L. T., "Results for a simple compact narrow-wall directional coupler," *IEEE Microwave and Guided Wave Letters*, Vol. 10, No. 6, 1051–8207, Jun. 2000.
19. Liu, B., W. Hong, Y. Zhang, J. X. Chen, and K. Wu, "Half-mode substrate integrated waveguide (HMSIW) double-slot coupler," *Electronics Letters*, Vol. 43, No. 2, 113–114, Jan. 18, 2007.
20. Ali, A., F. Coccetti, H. Aubert, and N. J. G. Fonseca, "Novel multi-layer SIW broadband coupler for nolen matrix design in Ku band," *IEEE/MTT-S International Microwave Symposium*, 1–4, 2008.
21. Labay, V. A. and J. Bornemann, "*E*-plane directional couplers in substrate-integrated waveguide technology," *Asia-Pacific Microwave Conference, APMC 2008*, 1–3, 2008.
22. Labay, V. A. and J. Bornemann, "Design of dual-band substrate-integrated waveguide *E*-plane directional couplers," *Asia Pacific Microwave Conference, APMC 2009*, 2116–2119, 2009.
23. Navarro, D. V., L. F. Carrera, M. Baquero-Escudero, and V. M. Rodrigo-Peñarrocha, "Compact substrate integrated waveguide directional couplers in Ku and K bands," *Proceedings of the 40th European Microwave Conference (2010 EuMA)*, 1178–1181, 2010.
24. Ali, A. A. M., H. B. El-Shaarawy, and H. Aubert, "Compact wideband double-layer half-mode substrate integrated waveguide 90° coupler," *Electronics Letters*, Vol. 47, No. 10, 598–599, May 12, 2011.
25. Chen, J. X., W. Hong, Z. C. Hao, H. Li, and K. Wu, "Development of a low cost microwave mixer using a broad-band substrate integrated waveguide (SIW) coupler," *IEEE Microwave Wirel. Compon. Lett.*, Vol. 16, No. 2, 84–86, 2006.